applied sciences

MDPI

Article

Morpho-Molecular and Genomic Characterization of *Penicillium mexicanum* Isolates Retrieved from a Forsaken Gold Mine

João Trovão [1,2,*], Fabiana Soares [1], Diana Sofia Paiva [1] and António Portugal [1,2,3,*]

[1] Centre for Functional Ecology (CFE)—Science for People & the Planet, Department of Life Sciences, University of Coimbra, Calçada Martim de Freitas, 3000-456 Coimbra, Portugal
[2] TERRA—Associate Laboratory for Sustainable Land Use and Ecosystem Services, Department of Life Sciences, University of Coimbra, Calçada Martim de Freitas, 3000-456 Coimbra, Portugal
[3] FitoLab—Laboratory for Phytopathology, Instituto Pedro Nunes (IPN), Rua Pedro Nunes, 3030-199 Coimbra, Portugal
* Correspondence: jtrovaosb@gmail.com (J.T.); aportuga@bot.uc.pt (A.P.)

Abstract: During the ongoing studies designed to examine the fungal diversity present within the abandoned and flooded Escádia Grande gold mine (Góis, Portugal), we repeatedly isolated several specimens belonging to a *Penicillium* species. Molecular phylogenetic analysis, coupled with morphological observations, positioned this fungus within subgen. *Penicillium* sect. *Paradoxa*, series *Atramentosa*, pinpointing its identity as *Penicillium mexicanum* (the first record for mining soils and the country). Given the limited research conducted on *Penicillia* isolated from similar environments, the species genome was sequenced utilizing the Oxford Nanopore® MinION™ methodology and studied through bioinformatic analysis. The obtained genome has a size of 29.62 Mb, containing a 47.72% GC content, 10,156 genes, with 44 rRNAs and 178 tRNAs/tmRNAs, providing the first genomic resource for this microorganism. Bioinformatic analysis allowed us to identify multiple genomic traits that can contribute towards this species survival in these extreme environments, including the presence of high levels of major facilitator transporters (MFS), Zn (2)-C6 fungal-type DNA-binding domains, P-loop containing nucleoside triphosphate hydrolases, specific fungal transcription factors and sugar transporters. Furthermore, putative advantageous metabolic traits, such as methylotrophy, assimilatory nitrate and sulfate reduction abilities, were also detected. In addition, the results also highlighted a strong genomic and metabolic organization and investment towards arsenic detoxification (transport and oxidation). Lastly, thirty-two putative biosynthetic gene clusters were predicted, including some with high similarity values to monascorubrin, nidulanin A, histidyltryptophanyldiketopiperazine/dehydrohistidyltryptophanyldiketopiperazine/roquefortine D/roquefortine C/glandicoline A/glandicoline B/meleagrine, YWA1 and choline. Overall, this study expands the current *Penicillia* knowledge from mining environments while also enhancing our understanding regarding fungal arsenic resistance.

Keywords: arsenic resistance; *Eurotiomycetes*; extreme environments; genomic analysis; gold mine mycobiome; *Penicillium mexicanum*

check for updates

Citation: Trovão, J.; Soares, F.; Paiva, D.S.; Portugal, A. Morpho-Molecular and Genomic Characterization of *Penicillium mexicanum* Isolates Retrieved from a Forsaken Gold Mine. *Appl. Sci.* **2024**, *14*, 10600. https://doi.org/10.3390/app142210600

Academic Editor: Ramona Iseppi

Received: 9 October 2024
Revised: 13 November 2024
Accepted: 14 November 2024
Published: 17 November 2024

Copyright: © 2024 by the authors. Licensee MDPI, Basel, Switzerland. This article is an open access article distributed under the terms and conditions of the Creative Commons Attribution (CC BY) license (https://creativecommons.org/licenses/by/4.0/).

1. Introduction

Regions with a history of auriferous mining activities are regarded as extreme ecological environments, predominantly due to the deleterious ecological ramifications that arise from these anthropogenic disturbances. The processes involved in gold extraction are responsible for the release and accumulation of heightened concentrations of heavy metals and metalloids, which can lead to environmental contamination and present a myriad of health hazards to humans [1–3]. The elevated levels of arsenic, along with other metals and metalloids in these areas, can impose selective pressures that favor the survival of distinct, resistant and well-adapted fungal species [4]. Nevertheless, mycological investigations within these environments have been pointed as being limited [4], and further research on

the fungal biodiversity, resistance traits and genomic characteristics in such settings, still needs to be thoroughly studied and documented.

The Fungal Kingdom comprises a vastly diverse collection of eukaryotic organisms, showcasing a broad range of morphological, ecological and metabolic traits that enables them to thrive in diverse environments across the planet. Owing to their distinctive features, fungi are recognized for their broad spectrum of biotechnological applications and valued for their sociological, ecological and economic significance [5–8]. The genus *Penicillium* represents one of the most globally prevalent fungal genera, inhabiting a wide array of ecosystems, including terrestrial substrates, vegetation, air, indoor spaces and a variety of alimentary products [9–11]. A substantial proportion of *Penicillium* species function as ubiquitous saprophytes, readily located in nearly any ecological niche [9]. They exhibit remarkable adaptability to diverse physical and chemical environments, which encompass a range of water activity (aW), pH, thermal gradients, environmental contaminants and redox potential variations. In addition, arsenic resistance within the genus has been documented, leading to its identification as integrant inhabitants of mining soil mycobiomes [4,12]. Owing to their metabolic capacities, *Penicillia* species have been reported as relevant microorganisms for the bioremediation of contaminated habitats, due to the ability of some species to tolerate and "remove" uranium, cadmium, lead and arsenic from the environment [4,13–17]. In addition, acid-tolerant and metal-resistant *Penicillia* are known to be key players in extreme environments, contributing to geochemical cycles and organic matter breakdown [16]. Moreover, some *Penicillium* species have been reported as holding some additional biotechnological interesting properties due to, for instance, their abilities for intra and extracellular biosynthesis of gold nanoparticles, which can have applications in the pharmaceutical and biomedical fields [18,19].

In an effort to contribute to the knowledge of abandoned gold mining areas microbial biodiversity, we have recently applied Next-Generation-Sequencing (NGS) methods to study the microorganisms thriving in the abandoned and flooded Portuguese Escádia Grande gold mine (Góis, Portugal) [20]. Moreover, in an attempt to shed light on the hidden fungal diversity in this area, we conducted a survey of culturable fungal species from soil/rocky materials from the mine interior. We have continuously isolated various specimens belonging to a *Penicillium* species during this investigation. The aim of this work was to determine the taxonomic position of this species, by employing a polyphasic approach consisting of phylogenetic analyses (β- tubulin (*BenA*), Internal Transcribed Spacer region (ITS rDNA), calmodulin (*CaM*) and the RNA polymerase II subunit 2 (*rbp2*)), coupled with morphological and ecological considerations. This analysis highlighted these isolates' identity as *Penicillium mexicanum* and allowed us to document some unreported morphological traits for this species. In addition, and to the best of our knowledge, this represents the first record of this species in the country and its retrieval from mining soils. Furthermore, given the lack of information for this species and for fungi retrieved from similar settings in general, we here report this microorganism's first Oxford Nanopore® MinION™ whole genome data and its peculiar associated genomic traits (including metabolic characteristics, arsenic resistance peculiarities and biosynthetic gene contents).

2. Materials and Methods

2.1. Fungal Isolation

Soil/rocky material samples were collected at about 1 m next to the entrance from the lateral carved rock/soil walls of the flooded Escádia Grande mine (Góis, Portugal) [20]. Approximately 25 g of soil were obtained from a depth ranging between 5 and 10 cm subsequent to the removal of the superficial 5 cm of soil and debris. Soil samples were air-dried for 24 h and then sieved before platting. Subsequently, the samples were suspended in 3 mL of sterile 0.9% (w/v) NaCl solution, vortexed thoroughly and plated onto Potato Dextrose Agar (PDA) (Difco, Franklin Lakes, NJ, USA) supplemented with streptomycin (0.5 g L^{-1}). Plate incubation was conducted over a span of thirty days at ambient temperature (25 $\pm$ 1 °C) and in complete darkness. Emerging *Penicillium* colonies were isolated to

fresh media plates and incubated until biomass had developed for further DNA extraction and morphological analysis preparation (7 days).

2.2. Morphological Characterization

For morphological analysis, the isolates were grown for 7 days at room temperature in PDA, malt-extract agar (MEA), dichloran glycerol agar (DG-18), czapek yeast autolysate agar (CYA), yeast extract sucrose agar (YES), unfiltered oatmeal agar (OA) and creatine sucrose agar (CREA). After incubation, traits such as sporulation levels, colony diameter, morphology and colors; mycelium color, texture and form; as well as the putative production of soluble pigments and the formation of exudates were evaluated. Microscopical morphological analysis was performed directly on the growing colonies or using the slide culture technique, with a light microscope (Leica DM750 (Leica, Wetzlar, Germany)) coupled to a digital camera (Leica ICC50W (Leica, Wetzlar, Germany)). In parallel, scanning electron microscopy (SEM) micrographs were taken with a Hitachi Flexsem 1000 variable-pressure microscope (Hitachi, Tokyo, Japan).

2.3. Phylogenetic Characterization

DNA from fungal cultures was obtained using the Extract-N-Amp™ Plant PCR Kit (Sigma Aldrich, St. Louis, MO, USA), with slight modifications as previously described [21]. The obtained DNA was subjected to PCR amplifications of the ITS rDNA using the universal primer pair ITS1-F/ITS4 [22,23]. The *rpb2* gene was amplified with the primer pair *RPB2*-5F/*RPB2*-7cR [24], the *CaM* gene with the primer pair CMD5/CMD6 [25] and the *BenA* gene with the primer pair Bt2a/Bt2b [26]. The PCR mixes comprised a total volume of 25 µL, consisting of 12.5 µL NZYTaq Green Master Mix (NZYTech™, Lisboa, Portugal), 1 µL of each primer (10 mM), 9.5 µL ultra-pure water and 1 µL of template DNA. The PCR programs involved an initial denaturation at 94 °C for 2 min, followed by 35 cycles of denaturation at 94 °C for 1 min, primer annealing at 55 °C for 1 min, primer extension at 72 °C for 90 s and a final extension step at 72 °C for 5 min [27]. PCR reactions were conducted using an ABI GeneAmp™ 9700 PCR System (Applied Biosystems, Carlsbad, CA, USA), and the resulting amplicons were purified and sequenced using an ABI 3730xl DNA Analyzer system (96 capillary instruments) at STABVIDA, Portugal.

DNA sequences were processed and assembled using the Geneious® R11.0.02 software (https://www.geneious.com), deposited in GenBank and initially compared with the sequences from the National Center of Biotechnology Information nucleotide databases using the NCBI Basic Local Alignment Search Tool (BLAST), with the option of Standard Nucleotide BLAST of BLASTN v.2.6 [28]. For construction of the datasets for phylogenetic analysis, additional reference sequences were retrieved from GenBank based on these preliminary results. To evaluate the isolate's phylogenetic position, a concatenated dataset of *BenA*, ITS rDNA, *CaM* and *rpb2* individual gene alignments based on the data presented in Houbraken and colleagues [9], Torres-Garcia and colleagues [29], Lee and colleagues [30] and Visagie and colleagues [11], was constructed. Moreover, an additional *BenA* sequence from one of the isolates was obtained by its extraction from its genomic data (see section below). Overall, the final dataset contained representative sequences of subgen. *Penicillium*, sect. *Turbata*, ser. *Turbata*, sect. *Paradoxa*, ser. *Atramentosa* and ser. *Paradoxa* (Table 1). Sequences of each gene were independently aligned using the online version of MAFFT v.7 [31], manually adjusted using UGENE v.1.26.3 [32] and concatenated using SeaView v.4 [33]. For phylogenetic analysis, the models of nucleotide substitutions were estimated with the ModelFinder software [34] associated with the W-IQ-TREE webserver [35] for each individual partition. Maximum likelihood (ML) phylogenetic analyses, as well as the Shimodaira-Hasegawa-like approximate likelihood ratio test (SH-aLRT) and approximate Bayes analysis (aBayes) [36,37], were conducted with W-IQ-TREE webserver (with 1000 bootstrap replicates to verify the branches when appropriate) [35]. The tree was rooted with representative sequences from sect. *Turbata*, ser. *Turbata*.

Table 1. Sequence data of *Penicillum* species used in the phylogenetic analyses. The new data generated during this study are pointed out in bold.

Species	Culture Collection [1]	GenBank Accession Numbers [2]			
		ITS	*BenA*	*CaM*	*rpb2*
Penicillium atramentosum	CBS 291.48	AF033483	AY674402	KU896821	JN406584
Penicillium balearicum	CBS 143044	LT899762	LT898227	LT899758	LT899760
Penicillium fimosum	CBS 142991	–	LT898273	–	–
Penicillium ibericum	CBS 142992	LT899782	LT898285	LT899766	LT899800
Penicillium magnielliptisporum	CBS 138225	KJ775686	KJ775179	KJ775413	MN969124
Penicillium mexicanum	CBS 138227	KJ775685	KJ775178	KJ775412	MN969127
Penicillium mexicanum	Y20P-5	OQ048471	OQ130423	OQ134945	–
Penicillium mexicanum	**MUM 23.42**	**PP376069**	**PP405214**	**PP421213**	**PP421215**
Penicillium mexicanum	**MUM 23.43**	**PP376070**	**PP405215**	**PP421214**	**PP421216**
Penicillium paradoxum	CBS 527.65	EF669707	EF669683	EF669692	EF669670
Penicillium crystallinum	CBS 479.65	AF033486	EF669682	FJ530973	EF669669
Penicillium malodoratum	CBS 490.65	AF033485	EF669681	FJ530972	EF669672
Penicillium sicoris	FMR 18076	LR884497	LR884494	LR884496	LR884495
Penicillium caprifimosum	CBS 142990	LT899781	LT898238	LT899765	LT899799
Penicillium bovifimosum	CBS 102825	AF263347	KJ834436	FJ530989	JN406649
Penicillium turbatum	CBS 383.48	AF034454	KJ834499	KU896853	JN406556
Penicillium madriti	CBS 347.61	AF033482	KJ834470	EU644076	JN406561

[1] CBS: Westerdijk Fungal Biodiverity Institute. FMR: Faculty of Medicine of Reus culture collection. MUM: Micoteca da Universidade do Minho. [2] *BenA*: β- tubulin. ITS: Internal Transcribed Spacer region. *CaM*: calmodulin. *rpb2*: RNA polymerase II subunit.

2.4. Genomic Characterization

High Molecular Weight (HMW) DNA extraction from *Penicillium mexicanum* MUM 23.42 was conducted utilizing the Nucleospin® Soil Kit (Macherey Nagel, Düren, Germany) in conjunction with Buffer SL2 and Enhancer SX, adhering to the manufacturer's protocols. The quantification of HMW DNA was executed using a Quantus fluorometer in conjunction with the QuantiFluor® dsDNA Dye kit (Promega, Madison, WI, USA) and subsequently evaluated through a 1% Tris-borate-EDTA (TBE) agarose gel electrophoresis, stained with GreenSafe Premium (NZYTech™, Lisboa, Portugal) and ran at 100 V for a duration of 45 min. Whole genome library preparation for Oxford Nanopore® MinION™ sequencing was performed utilizing the Rapid Barcoding Kit 24 V14 (SQK-RBK114.24), following the manufacturer's protocol. The library was subsequently loaded into a R10.4.1 flow cell (FLO-MIN114) and sequenced using a MinION™ Mk1B connected to a portable ASUS TUF Gaming A16 (FA607PV-R97B46CS1) laptop over a period of 36 h. Data processing analysis was performed with the MinKnow software v.24.06.5. Read basecalling was carried out employing the Super accurate (SUP) model with Guppy v.6.5.7, whereby barcodes and reads exhibiting a mean quality lower than 10 and with lengths less than 1000 bp were excluded from the dataset.

The web-based Galaxy platform [38] was utilized for bioinformatic analysis. To evaluate the quality of initial reads and overall metrics, the NanoPlot v.1.43 [39] software was employed. Nanopore raw reads underwent assembly via the Flye assembler v.2.9.5 [40], utilizing the options—nano-raw—scaffold and conducting three internal rounds of self-polishing. The final assembly underwent evaluation with Quast v.5.2.0 [41] and gfastats v.1.3.6. Genome completeness was assessed using the Benchmarking Universal Single-Copy Orthologs (BUSCO) v.5.7.1 [42], employing the ortholog dataset designated for *Eurotiales* (orthoDB v.10) [43]. Genomic ribosomal RNA genes were identified utilizing Barrnap v.1.2.2 [44], while tRNA genes were detected with ARAGORN v.1.2.36 [45]. Repetitive elements were detected and soft-masked employing RepeatModeler v.2.0.5 [46] and RepeatMasker v.4.1.25 [47], with the genome annotation being performed with the Funannotate pipeline v.1.8.15. Coding genes underwent further functional annotation with the UniProtKB Swiss-Prot database (UniProt Consortium, 2017), the EggNOG Mapper v.2.1.8 [48] and InterProScan v.5.59-91.0 [49,50]. The OmicsBox software v.3.2.2 was employed to execute

Blast2Go analysis [51,52] to acquire InterPro protein information, combine Gene Ontology (GOs) terms, and perform GOSlim and enzyme mapping analysis. Carbohydrate-active enzymes were identified utilizing the dbcan3 web-server [53], while biosynthetic gene clusters (BGCs) were scrutinized using the antiSMASH web server v.7.1.0 [54]. Furthermore, the BlastKoala mapping tool [55] was employed to reconstruct metabolic pathways and correlate the function of each gene product against the Kyoto Encyclopedia of Genes and Genomes (KEGG). The AsgeneDB [56] was screened with DIAMOND v.2.0.15 [57] (identity = 50%, evalue < 10^{-4}), in order to obtain information regarding the species arsenic resistance gene contents and metabolic peculiarities. Additional data visualization and plotting were conducted using SRPlot [58].

3. Results and Discussion

3.1. Phylogenetic Analysis

The phylogenetic analysis was performed with the combined four-gene dataset consisting of 1913 characters and encompassing representative sequences belonging to *Penicillium* subgen. *Penicillium*, sect. *Turbata*, ser. *Turbata*, sect. *Paradoxa*, ser. *Atramentosa* and ser. *Paradoxa*. The phylogenetic inferences based on this combined dataset showed that the sequences obtained during this study clustered in a monophyletic group with strong support, identified as consisting of *Penicillium mexicanum* representative strains (Figure 1).

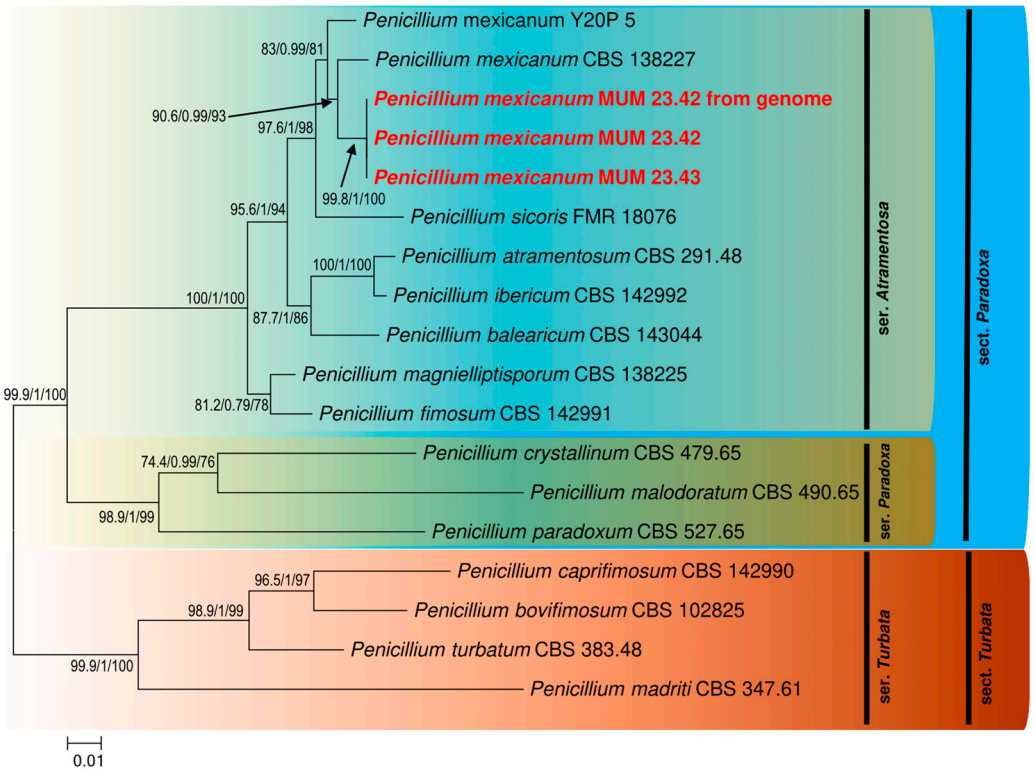


Figure 1. Phylogenetic tree obtained from the aligned concatenated four-gene dataset. The data obtained in this work are highlighted in red and bold. The scale bar indicates the number of substitutions per site, and the support values (SH-aLRT/aBayes/ML) are also shown.

3.2. Morphological Analysis

Taxonomy

Penicillium mexicanum Visagie, Seifert and Samson, Studies in Mycology 78: 125. 2014 [59]. MycoBank: MB 809185. Figures 2 and 3 and Supplementary Figure S1.

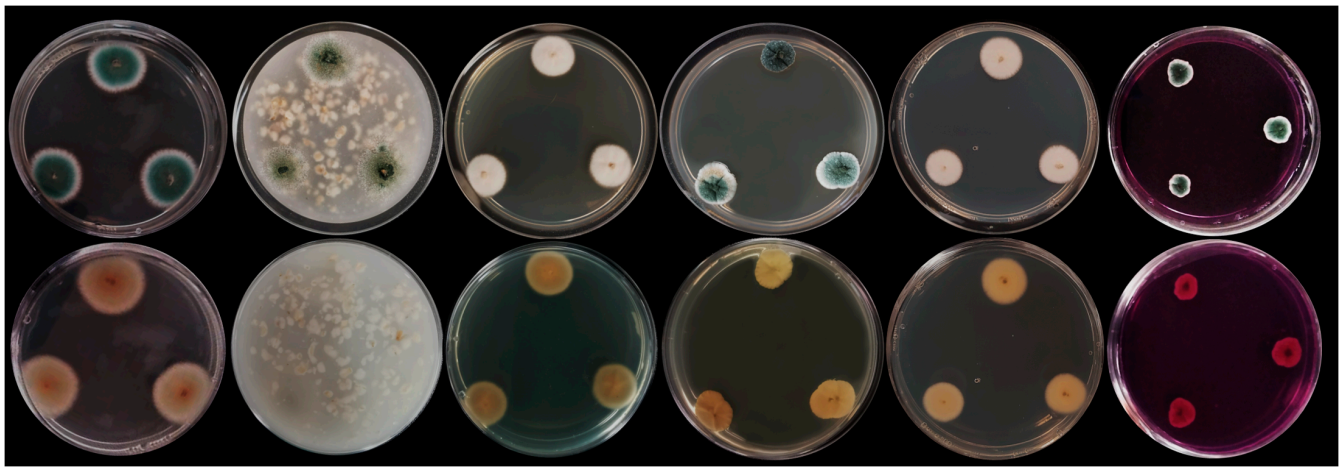


Figure 2. *Penicillium mexicanum* MUM 23.42 colony characteristics (averse above, reverse bellow) after 7 days in (from left to right) MEA, OA, CYA, DG-18, YES and CREA.

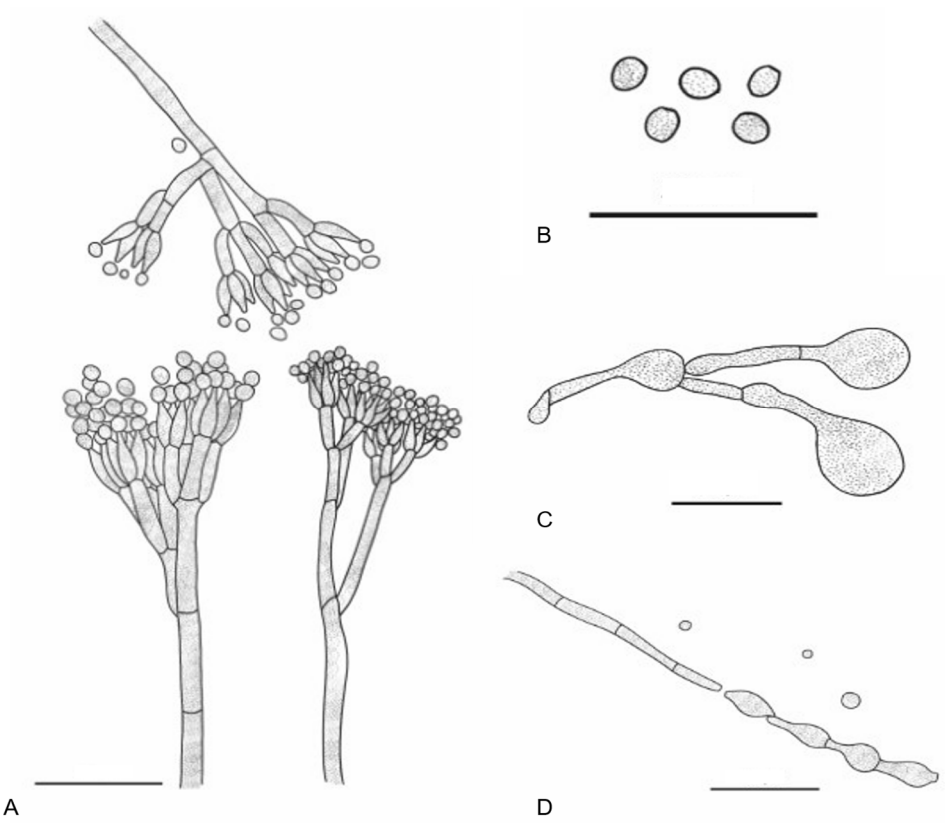


Figure 3. Drawing details of *Penicillium mexicanum* MUM 23.42: (**A**) Conidiophores. (**B**) Conidia. (**C**,**D**) Chains of chlamydospores. Scale bar = 20 μm (**A**–**D**).

Specimens examined: Portugal, Coimbra, Góis, 40°04′50.0″ N, 8°06′57.0″ W, isolated from soil/rocky debris from an abandoned gold mine, 17 November 2021, J. Trovão, MUM 23.42; ibid MUM.23.43.

Culture characteristics: Colonies on MEA after 7 days at 25 °C, reaching up to 13.5 mm, flat, velvety to floccose, olive to dark green at the center and white in the margins, margins narrow (2.5–3.5 mm), low, entire, sporulation abundant, conidia *en masse* olive green. Reverse reddish to brown at the center, dull white at the edge. Exudates and soluble pigments absent. Colonies on OA after 7 days at 25 °C, reaching up to 13 mm, raised at the center, velvety to floccose, dark green at the center, becoming white towards the

periphery, margins wide (2.5–5 mm), low, slightly undulate, sporulation abundant at the center, conidia *en masse* dark green. Reverse pale green at the center, dull white at the edge. Exudates and soluble pigments absent. Colonies on CYA after 7 days at 25 °C, reaching up to 10.5 mm, flat, velvety, cream white, margins narrow (2–3 mm), low, entire, sporulation scarce. Reverse light brown at the center, dull white at the edge. Exudates and soluble pigments absent. Colonies on DG-18 after 7 days at 25 °C, reaching up to 12 mm, raised at the center, sulcate, velvety to floccose, olive to dark green at the center and white in the margins, margins wide (1–5 mm), low, entire, sporulation abundant, conidia *en masse* dark green. Reverse reddish to brown at the center, dull white at the edge. Strong production of hyaline exudates, soluble pigments absent. Colonies on YES after 7 days at 25 °C, reaching up to 10.5 mm, flat, velvety, cream white, margins narrow (2–3 mm), low, entire, sporulation scarce. Reverse dull white. Exudates and soluble pigments absent. Colonies on CREA after 7 days at 25 °C, reaching up to 8.5 mm, raised at the center, slightly sulcate, velvety to floccose, margins wide (1–1.5 mm), low, slightly undulate, sporulation abundant, conidia *en masse* olive green. Reverse reddish to brown at the center, dull white at the edge. Exudates and soluble pigments absent, no acid production. When considering longer incubation periods, strong acid production detected.

Micromorphological characteristics: Hyphae hyaline to subhyaline, smooth, thin-walled, 3–4 µm wide. Conidiophores divaricate, biverticillate or terverticilliate, stipes smooth-walled, 11.5–60 ($\overline{X}$ = 31.4; SD = 15.3) × 2.5–7.5 ($\overline{X}$ = 3.5; SD = 1.1) µm, metulae appressed to divergent, 3–4 per branch, 5–14.5 ($\overline{X}$ = 7.7; SD = 2.17) × 1.5–4 ($\overline{X}$ = 2.65; SD = 0.59) µm, phialides 2–4 per metula, ampulliform, 5–7.5 ($\overline{X}$ = 6.03; SD = 0.74) × 1.5–3.5 ($\overline{X}$ = 2.3; SD = 0.52) µm. Conidia one-celled, subhyaline to greenish, smooth, broadly ellipsoidal, 2.5–3.5 ($\overline{X}$ = 2.6; SD = 0.43) µm × 1.5–2.5 ($\overline{X}$ = 1.8; SD = 0.3) µm. Hyaline chlamydospores, smooth, solitary and in chains, intercalary and terminal, irregular, subglobose to globose 3.5–17.5 ($\overline{X}$ = 8.6; SD = 3.95) µm × 3.5–14.5 ($\overline{X}$ = 8.5; SD = 3.58) µm, with smooth cell wall 1.05–1.65 ($\overline{X}$ = 1.35; SD = 0.31) µm thick. Sexual morph not detected.

GenBank barcodes: MUM 23.42 ITS: PP376069; *BenA*: PP405214; *CaM*: PP421213; *rpb2*: PP421215. MUM 23.43 ITS: PP376070; *BenA*: PP405215; *CaM*: PP421214; *rpb2*: PP421216.

Series *Atramentosa* is characterized by moderately fast-growing colonies, brown reverse color on CYA and YES, velvety colony textures, predominantly terverticillate conidiophores with smooth-walled globose to subglobose or (broadly) ellipsoidal conidia and good growth on CREA, without acid production [9,11,29]. Nonetheless, morphological and phenotypic variation for this species has been reported in the pass [30]. Accordingly, the isolates studied exhibited light brown reverse colors on CYA [9,29]. However, on YES, the studied isolates are reverse dull white, while per the *P. mexicanum* type description, they are commonly dull yellow/olive [9,29]. Moreover, the studied isolates presented somewhat relatively smaller conidia sizes (3–4 × 3–3.5 µm in *P. mexicanum* type). In addition, the studied isolates differ from the typical displayed *P. mexicanum* characteristics by the strong production of hyaline exudates on DG-18 and the presence of chlamydospores.

So far, *Penicillium mexicanum* has been detected in house dust, air and intertidal zones (mudflats and sands) [29,30,59,60], with the results obtained during the course of this work pointing (to the best of our knowledge) for its first detection in Portugal and in soil samples from mining areas. Substrates such as mines, mining areas and acid mine drainage (AMD) ecosystems have been poorly studied so far, at least from a mycological perspective. They require additional focus, since underexplored substrates and extreme environments have been recently highlighted to contain unexpected high degrees of fungal diversity [61,62]. *Penicillia* ability to withstand extreme environments is linked to their halophilic/halotolerant, osmophilic/osmotolerant and xerophilic/xerotolerant characteristics [62]. When considering gold mines, arsenic resistance has also been highlighted as a key metabolic feature contributing towards *Penicillium* successful survival at these sites [4]. This is a result of arsenic being frequently associated with gold extraction, being a common metalloid polluting gold mining areas. Further studies focusing on *Penicillia* and related genera from mining soils and related substrates are crucial as these fungi can

also hold additional biotechnological potential (see below), considering their wide range of applications on areas such as the bioremediation of soils, tailings and water; biomining, bioleaching and the biosynthesis of gold nanoparticles (e.g., [13–19]). These bioprocesses are not restricted to Bacteria or Archaea, and some extremophile fungi can also play an important role in these interactions with minerals and mining ores.

3.3. Genomic Characteristics

In total, 155,957 quality reads were assembled in 22 scaffolds consisting of 29,620,091 bp (30× average coverage; circularization achieved for one scaffold (mitochondrial genome); a GC content of 47.72%; Scaffold N50 of 4,060,673; an average scaffold length of 1,346,367.77; and the largest scaffold being 8,180,881 bp) (Table 2). The Funannotate, Barrnap, and ARAGORN software's predicted the occurrence of 10156 coding genes, with forty-four rRNAs (two 18S rRNAs, three 28S rRNAs (one solely partial), two 5.8S rRNAs and thirty and seven 5S rRNAs) and one hundred and seventy-eight tRNAs. The Benchmarking Universal Single-Copy Orthologs (BUSCO) completeness was estimated to be at 99.6% for *Eurotiales* (*n* = 4191), with 4174 complete BUSCOs, 4167 complete and single-copy BUSCOs, 7 complete and duplicated BUSCOs, 5 fragmented BUSCOs and 12 missing BUSCOs (Figure 4).

Table 2. Overall genome assembly metrics.

Info	Value
Scaffold number	22
Total scaffold length	29,620,091
Average scaffold length	1,346,367.77
Scaffold N50	4,060,673
Scaffold auN	4,720,784.16
Scaffold L50	3
Largest scaffold	8,180,881
Smallest scaffold	7668
N's number	0
Read mean quality	14.1
Read median quality	17.2
Initial number of reads	155,957
Read mean quality	14.1

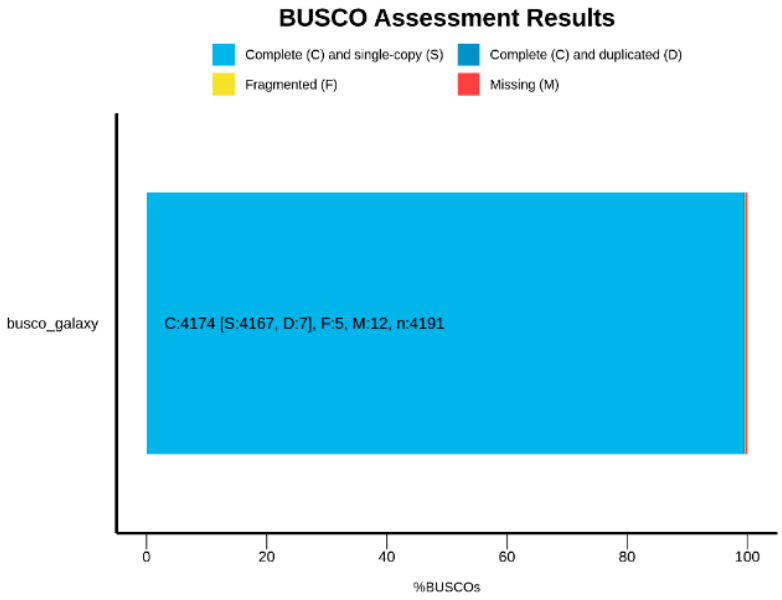


Figure 4. Genome completeness as evaluated with BUSCO and the *Eurotiales* database (orthoDB v.10).

Petersen and colleagues [63] conducted the largest study focusing on *Penicillium* genomic characteristics with the Oxford Nanopore® sequencing methodology to date (93 isolates). They found that the estimated genomic sizes and gene numbers ranged from 25.4 to 46.5 Mb and contained 9591–14,319 coding genes, with an array of contigs/scaffolds being between 5 and 65. Thus, the results obtained during the course of this work can be considered to be within the typical average ranges for the genus (29.6 Mb, 10,156 coding genes and 22 scaffolds). Currently, more than 400 *Penicillium* genomes are publicly available [64]; yet, to the best of our knowledge, no genomic data exist neither for this species and neither for sect. *Paradoxa*, ser. *Atramentosa*.

The functional genomic analysis based on the conducted annotation (Supplementary Table S1; Figure 5) pointed out that the top five most representative domains for (1) biological processes were as follows: the regulation of cellular process, cellular process, the positive regulation of cellular process, response to stress and the positive regulation of transcription by RNA polymerase II; (2) the cellular components were as follows: cytoplasm, cytosol, nucleus, membrane and plasma membrane; and (3) the molecular functions were as follows: protein binding, binding, identical protein binding, metal ion binding and ATP binding. These findings underscore a significant representation of biological, cellular and molecular traits associated with the regulation of cellular processes and transmembrane transport, as well as protein, metals and ATP binding functions. Somewhat similar results were reported by Roxo and colleagues [65] for the genome of *Penicillium pancosmium* MUM 23.27 (isolated from raw honey) and could be a result from their survival needs in unusual extreme environments.

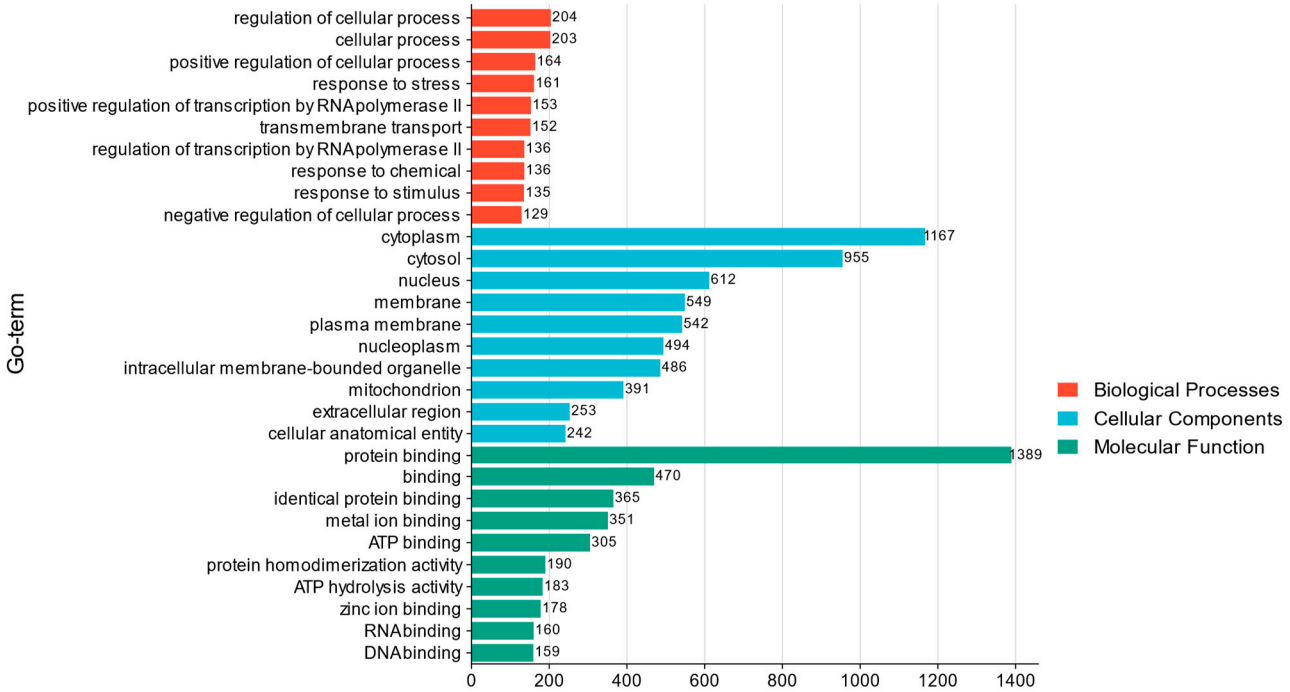


Figure 5. Gene Ontology (GO) terms count for the top 10 most representative GO terms (i.e., for biological processes, cellular components and molecular function) in the genome annotation.

InterProScan predicted the presence of 4482 protein families, 2929 protein domains, 424 protein sites and 62 protein repeats. The top five most representative (1) families were as follows: (IPR027417) P-loop containing nucleoside triphosphate hydrolase, (IPR036259) MFS transporter superfamily, (IPR036291) NAD(P)-binding domain superfamily, (IPR011009) protein kinase-like domain superfamily and (IPR011701) major facilitator superfamily; (2) the domains were as follows: (IPR020846) major facilitator superfamily domain, (IPR001138) Zn(2)-C6 fungal-type DNA-binding domain, (IPR007219) transcription factor domain, fungi, (IPR000719) protein kinase domain and (IPR003593) AAA+ ATPase domain; (3) the sites

were as follows: (IPR008271) serine/threonine-protein kinase, active site, (IPR005829) sugar transporter, conserved site, (IPR017441) protein kinase, ATP binding site, (IPR020904) short-chain dehydrogenase/reductase, conserved site and (IPR019775) WD40 repeat, conserved site; and (4) the repeats were as follows: (IPR001680) WD40 repeat, (IPR002110) ankyrin repeat, (IPR019734) tetratricopeptide repeat, (IPR020472) G-protein beta WD-40 repeat and (IPR018108) mitochondrial substrate/solute carrier (Figure 6). In previous works [65–67], high levels of major facilitator transporters (MFS), Zn (2)-C6 fungal-type DNA-binding domains (IPR001138), fungal transcription factor domain (IPR007219) and sugar transporters conserved sites (IPR017441), have been found to be sturdily represented in stress-tolerant or adapted fungal species, such as *Hortaea werneckii*, *Friedmanniomyces endolithicus*, *Aeminium ludgeri*, *Saxispiralis lemnorum* and *Penicillium pancosmium*. They have been commonly associated with the transportation of small solutes in response to chemiosmotic ion gradients, resistance to toxic compounds and allow the functionality of metabolic systems in extreme environments [65–68]. Their detection is, thus, in line with common responses to the environment from where the *Penicillium mexicanum* strains were retrieved. Moreover, the dominant presence of (IPR027417) P-loop containing nucleoside triphosphate hydrolase is also relevant since multiple NTPases are metalloenzymes/metallochaperones interacting and transporting metal ions [69] and can consequently play important roles towards the proper cell functioning of *Penicillium mexicacum* in these contaminated environments.

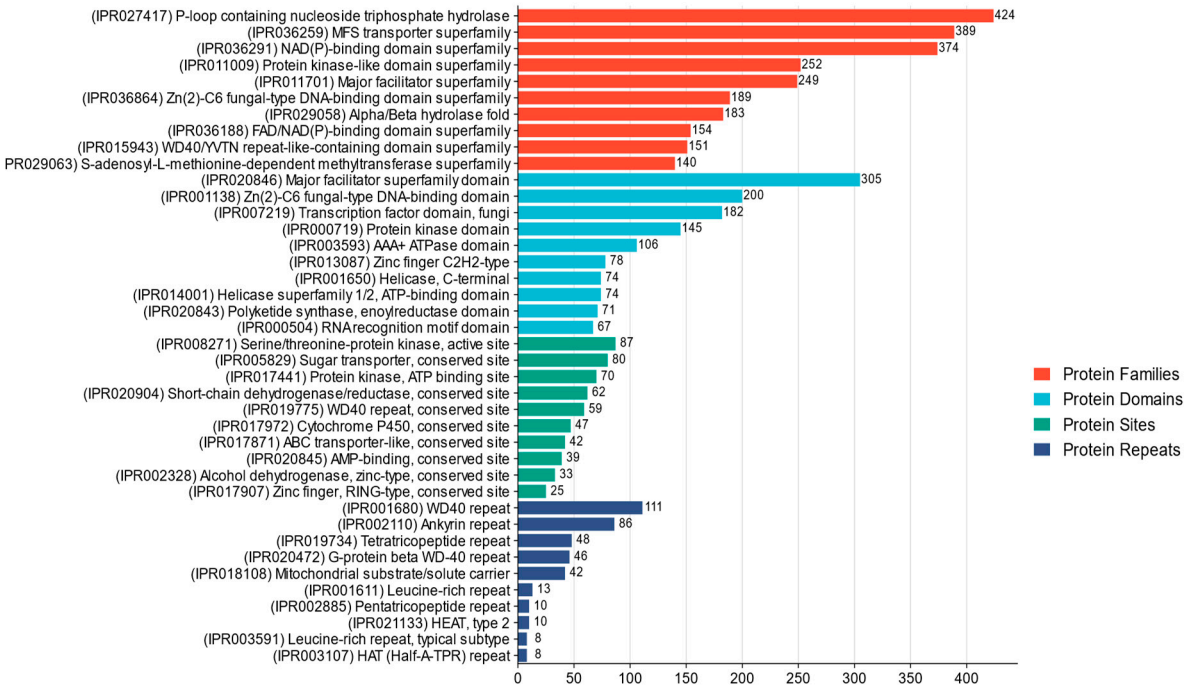


Figure 6. InterProScan terms count for the top 10 most representative protein families, domains, sites and repeats found in the genome annotation.

The OmicsBox enzyme coding mapping tool highlighted that the most prevalent enzyme types predicted in the genome were hydrolases, transferases and oxidoreductases (Supplementary Table S2). In parallel, the Eggnog mapper revealed that the top five most relevant Clusters of Orthologous Genes (COGs) category groups were as follows: [S] function unknown, [G] carbohydrate transport and metabolism, [E] amino acid transport and metabolism, [O] post-translational modification, protein turnover, chaperones and [U] intracellular trafficking, secretion, and vesicular transport (Figure 7). The high number of hydrolases, transferases and oxidoreductases, coupled with a strong representation of [G] carbohydrate transport and metabolism and [E] amino acid transport and metabolism, highlights both the species saprotrophic nature but also the main metabolic features and requirements contributing to their survival in mining soils.

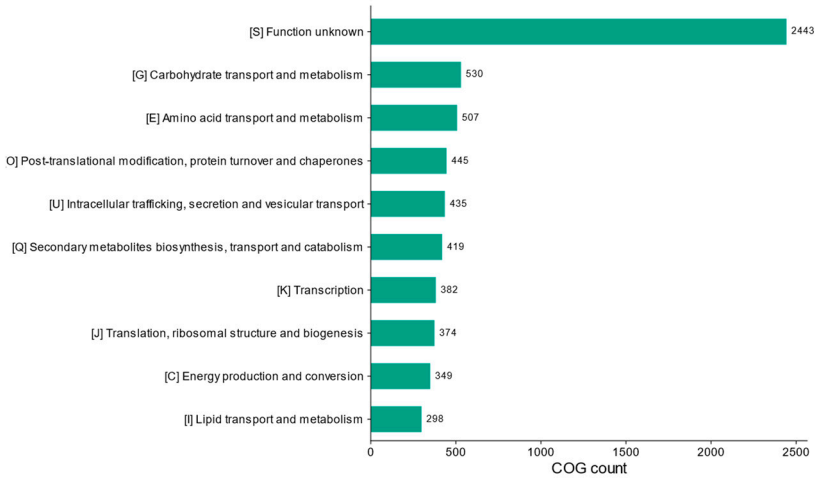


Figure 7. Eggnog mapper top 10 Clusters of Orthologous Genes (COGs) categories count for the studied genome annotation.

Complementarily, the dbCAN3 software identified 1694 carbohydrate-active enzymes (CAZomes), with a high dominance of glycoside hydrolases (GHs) and glycosyltransferases (GTs); intermediary numbers for auxiliary activities (AAs), carbohydrate-binding modules (CBMs) and carbohydrate esterases (CEs); and rather low numbers of polysaccharide lyases (PLs) (Supplementary Table S3). The dominance of GT2, GH3 and AA3_2 (Figure 8) was also reported for *Penicillium pancosmium* MUM 23.27 [65] and can highlight a strong metabolic focus on the biosynthesis of structural fungal cell wall polysaccharides (such as chitin and glucan) (GT2); the degradation of plant biomass, particularly complex carbohydrates such as cellulose and hemicellulose (GH3); and the breakdown of lignin (laccases) or the enhancement other lignocellulolytic enzymes (AA3_2).

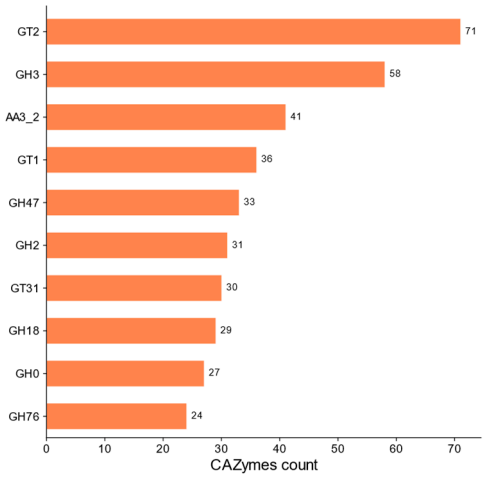


Figure 8. dbCAN3 top 10 carbohydrate-active enzymes counts found in the genome annotation.

The fungal antiSMASH tool predicted the presence of thirty-two putative biosynthetic gene clusters (BGCs) in the genome. From these, nine were T1PKS, five were NRPS, an additional five were NRPS-like, three were terpenes, two were NRPS, T1PKS and various single detections of betalactones; fungal-RiPP-like; indole, NRPS; NRP-metallophore, NRPS; NRPS-like, fungal-RiPP-like; NRPS-like, T1PKS; T1PKS, indole and T1PKS, NRPS-like, were also detected. The most relevant and found to hold a higher similarity (>75%) with the MiBiG database pertained to the presence of monascorubrin, nidulanin A, histidyltryptophanyldiketopiperazine/dehydrohistidyltryptophanyldiketopiperazine/roquefortine D/roquefortine C/glandicoline A/glandicoline B/meleagrine, YWA1 and choline (Table 3).

Interestingly, a possible homolog for penicillin was also detected in the genome (although with low similarity values) (Table 3 and Figure 9). Recently, the genus *Penicillium* has been identified as producing some of the most diverse groups of metabolites [70], and the data obtained during the course of this work are in accordance with this observation. Moreover, monascorubrin is a colored polyketide belonging to a class of pigments, known as azaphilones, that possess both coloring and bioactive properties [71,72]. Nidulanin A represents a cyclic tetrapeptide that is frequently identified within the genera *Aspergillus* and *Penicillium* [65,73], for which their biological features are not yet deeply characterized. Regarding the identified histidyltryptophanyldiketopiperazine/dehydrohistidyltryptophanyldiketopiperazine/roquefortine D/roquefortine C/glandicoline A/glandicoline B/meleagrine BGC, they are known to be involved in the synthesis of mycotoxins with some pharmaceutically interesting properties, but they also present some challenges in the food industry [74–76]. On the other hand, YWA1 is classified as a naphthopyrone pigment and is recognized as a precursor in the biosynthetic pathway of 1,8-dihydroxynaphthalene (DHN)-melanin production [77–79]. Furthermore, choline serves as a precursor for the production of phospholipids allowing the maintenance of cell membranes, with their derivates being known to be involved in osmotolerance mechanisms in some *Penicillium* species [80]. Both the presence of YWA1 and choline reinforces a strong focus in the species survival in harsh environments, since they can function as multifaceted protectors against environmental stressors (e.g., [81,82]). Further studies regarding the synthesis mechanisms and the identity of the possible penicillin homolog, but also from the additional BGCs, remain pending and should be encouraged due to their putative pharmaceutical and biotechnological potentials.

Table 3. antiSMASH predicted BGCs in the studied genome.

Region	Type	Most Similar Known Cluster	Similarity (%)
Region 2.1	NRPS	penicillin	18%
Region 3.1	T1PKS, NRPS-like	lucilactaene	23%
Region 3.2	T1PKS		
Region 3.3	T1PKS		
Region 3.4	terpene	squalestatin S1	60%
Region 3.5	NRPS, T1PKS	equisetin	18%
Region 3.6	T1PKS	andrastin A	40%
Region 3.7	NRPS		
Region 3.8	NRP-metallophore, NRPS		
Region 3.9	T1PKS	monascorubrin	100%
Region 3.10	NRPS-like, T1PKS		
Region 4.1	NRPS-like		
Region 4.2	NRPS-like		
Region 7.1	T1PKS	gregatin A	44%
Region 7.2	NRPS		
Region 7.3	terpene		
Region 7.4	T1PKS		
Region 7.5	NRPS	nidulanin A	75%
Region 7.6	fungal-RiPP-like		
Region 12.1	indole, NRPS	histidyltryptophanyldiketopiperazine/ dehydrohistidyltryptophanyldiketopiperazine/ roquefortine D/roquefortine C/ glandicoline A/glandicoline B/ meleagrine	100%
Region 12.2	NRPS, T1PKS	YWA1	100%
Region 12.3	NRPS-like	choline	100%
Region 18.1	T1PKS		
Region 20.1	T1PKS, indole		
Region 20.2	NRPS-like		
Region 20.3	betalactone		
Region 21.1	NRPS-like, fungal-RiPP-like	atpenin B	54%
Region 21.2	NRPS		
Region 21.3	NRPS-like		
Region 21.4	T1PKS		
Region 21.5	terpene		
Region 21.6	T1PKS	4-epi-15-epi-brefeldin A	20%

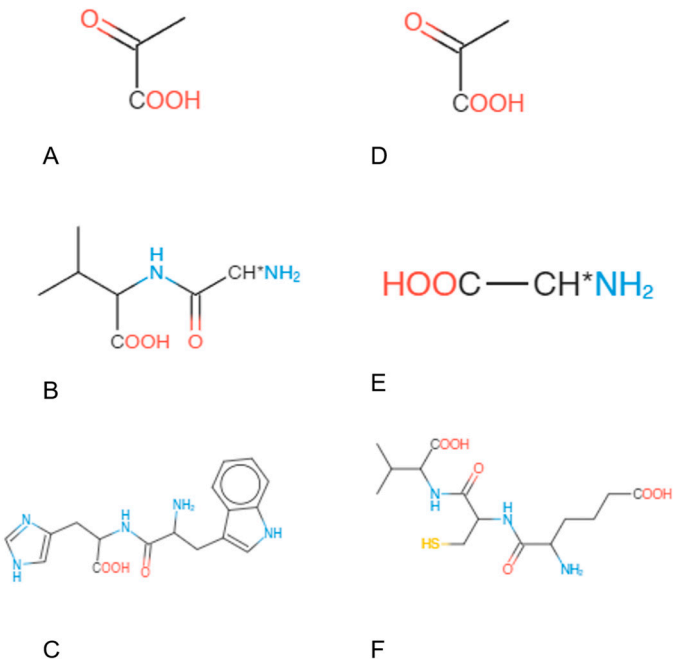


Figure 9. Predicted structures of: (**A**) monascorubrin, (**B**) nidulanin A, (**C**) histidyltryptophanyldiketopiperazine/dehydrohistidyltryptophanyldiketopiperazine/roquefortine D/roquefortine C/glandicoline A/glandicoline B/meleagrine, (**D**) YWA1, (**E**) choline and (**F**) the penicillin homolog.

BlastKoala annotated 3949 coding genes (38.9%), with the most relevant results highlighting the species ability for assimilating formaldehyde through the xylulose monophosphate pathway or dihydroxyacetone cycle (methane metabolism and methylotrophy) (M00344; complete); nitrate assimilation (signature module set) assimilating nitrate through the assimilatory nitrate reduction into ammonia (M00615; complete); assimilatory sulfate reduction (sulfur metabolism), converting sulfate to sulfide (H_2S) (M00176; complete); and the ability of the fungus to synthetize beta-lactams, namely, penicillin, through the pathway aminoadipate + cycteine + valine => penicillin (M00672; complete). Methylotrophic microorganisms exhibit the unique capacity to utilize single-carbon substrates, encompassing methane, methanol, formate and carbon monoxide as their primary carbon source for proliferation. The capability for methylotrophic metabolism may provide a considerable benefit, especially in extreme habitats, since they allow these microorganisms to survive and develop in conditions characterized by nutrient scarcity [83,84]. In fact, fungal methylotrophy could enhance their survival in extreme conditions while also contributing to the detoxification of toxic compounds, the support of carbon cycling and potentially influencing biomineralization processes. On the other hand, in arsenic-rich mine soils, fungal assimilatory nitrate and sulfate reduction might not only promote basic metabolic functions like nitrogen and sulfur acquisition but also contribute to the detoxification and maintenance of cellular homeostasis under extreme environmental stress. Oxidative stress causing the disruption of cellular processes and increase in reactive oxygen species (ROS) can be mitigated by the tight regulation of nitrogen metabolism through antioxidant production, such as glutathione, and by binding arsenic into less toxic forms. Complementarily, assimilatory sulfate reduction ensures the synthesis of cysteine and methionine, critical for the formation of glutathione and allowing for arsenic detoxification, while also permitting the direct interaction of sulfide with arsenic to form insoluble arsenic sulfides (e.g., arsenopyrite), thereby lowering arsenic's bioavailability and toxicity. In fact, from the KEGG analysis for the metabolism of other amino acids, glutathione metabolism was the most represented pathway (17 entries) reinforcing this assumption. In addition, the KEGG analysis of the reactive oxygen species pathway (mapped in chemical carcinogenesis) revealed the microorganism's ability to detoxify arsenic through the antioxidant

defense system and the action of arsenite methyltransferase [EC:2.1.1.137], glutathione S-transferase [EC:2.5.1.18], arsenite methyltransferase [EC:2.1.1.137], NADH-ubiquinone oxidoreductase chain 1 [EC:7.1.1.2], succinate dehydrogenase (ubiquinone) flavoprotein subunit [EC:1.3.5.1], ubiquinol-cytochrome c reductase iron–sulfur subunit [EC:7.1.1.8], cytochrome c oxidase subunit 3, F-type H^+-transporting ATPase subunit alpha, superoxide dismutase, Fe-Mn family [EC:1.15.1.1], voltage-dependent anion channel protein 1, superoxide dismutase, Cu-Zn family [EC:1.15.1.1] and catalase [EC:1.11.1.6]. The additional screening of the AsgeneDB database also revealed some peculiarities related to arsenic resistance, namely, the presence of specific genes, such as ACR3 (12 count), GET3 (8 count) and arsB (4 count) [all are As(III) efflux pump/permeases for detoxification]; ACR2 (1 count) and GstB (3 count) [both can conduct the reduction of As(V) to As(III) that can be excreted through the As(III) efflux pumps]; arsM (6 count) [As(III) sadenosylmethionine (SAM) methyltransferase (arsM)]; arsH (2 counts) [methylarsenite-specific oxidase (ArsH) that can oxidize methylarsenite to methylarsenate]; and pstB (6 count), glpF (1 count) and PiT (1 count) [all are glycerol phosphate transporters that can absorb As(III) and As(V)] [56,85]. These results reinforce the strong genomic and metabolic organization and investment towards *Penicillium mexicacum* arsenic transport and As (III) oxidation.

In parallel, multiple siderophores (iron transporters), siderochromes (iron transporters), iron–sulfur cluster transporters and various other iron-related proteins were also detected in the genome annotation (Supplementary Table S1), also suggesting that they are essential for *Penicillium mexicacum* survival, the maintenance of normal metabolic function and resistance to metal toxicity in these contaminated environments. In fact, the production of siderophores, siderochromes and metal-chelating compounds allows for fungal survival in extreme environments where nutrients are scarce, while also ensuring the neutralization of toxic metals [86–89]. Complementarily, iron–sulfur clusters also facilitate the survival and adaptation to metal-rich environments, partaking in critical roles for fungal homeostasis such as electron transport processes, nitrogen fixation, sulfur assimilation, amino acid biosynthesis, ROS detoxification and DNA repair [89,90].

4. Conclusions

This study reports the first documentation of *Penicillium mexicanum* from an abandoned and flooded gold mine in Portugal. Morphological and micromorphological examinations elucidated various distinctive attributes, such as the presence of chlamydospores and hyaline exudates, that may reflect adaptations to the environmental conditions prevalent in the studied mining soil substrates. The genomic examination of the analyzed *P. mexicanum* strains disclosed a broad spectrum of metabolic pathways, particularly those associated with cellular stress response and transmembrane transport, which are likely instrumental in facilitating the species' resilience within metal-contaminated habitats. Moreover, the identification of several BGCs, including those reflecting adaptations to harsh environment and those holding prospective biotechnological implications, are also relevant for expanding *Penicillia* biological knowledge. Nonetheless, additional inquiries into this species and other extremophilic fungi inhabiting analogous environments are imperative to fully elucidate their biotechnological potential and applications while also accentuating the need to investigate underexplored and extreme ecosystems to further understand their diversity and metabolic properties.

Supplementary Materials: The following supporting information can be downloaded at https://www.mdpi.com/article/10.3390/app142210600/s1. Supplementary Table S1: Overall genome annotation; Supplementary Table S2: Enzyme classes and subclasses detected; Supplementary Table S3: Overall dbcan3 results. Supplementary Figure S1: *Penicillium mexicanum* MUM 23.42: A–C. Terverticillate conidiophores. D. Conidia. E–F. Terminal and intercalary chlamydospores. G. Details of hyaline exudates detected on DG-18. Scale bar = 20 µm (C–F), 30 µm (A) and 50 µm (B).

Author Contributions: Conceptualization, J.T.; methodology, J.T., F.S. and D.S.P.; formal analysis, J.T.; investigation, J.T., F.S. and D.S.P.; resources, J.T. and A.P.; writing—original draft preparation, J.T.;

writing—review and editing, all authors; supervision, J.T. and A.P.; funding acquisition, J.T. and A.P. All authors have read and agreed to the published version of the manuscript.

Funding: This work was carried out at the R&D Unit Centre for Functional Ecology—Science for People and the Planet (CFE) and Associate Laboratory TERRA. The Centre for Functional Ecology—Science for People and the Planet (CFE) was supported by FCT—Fundação para a Ciência e Tecnologia, I.P.—by project reference UIDB/04004/2020 and the DOI identifier 10.54499/UIDB/04004/2020 (https://doi.org/10.54499/UIDB/04004/2020). The Associate Laboratory TERRA was supported by FCT—Fundação para a Ciência e Tecnologia, I.P.—by project reference LA/P/0092/2020 and the DOI identifier 10.54499/LA/P/0092/2020 (https://doi.org/10.54499/LA/P/0092/2020). The authors also thank the funding of PRR—Recovery and Resilience Plan—and the NextGeneration EU European Funds. Diana Paiva was supported by a PhD research grant (UI/BD/150843/2021) awarded by the Centre for Functional Ecology—Science for People and the Planet (CFE) and co-funded by Fundação para a Ciência e Tecnologia, I.P. (FCT) through national funding by the Ministério da Ciência, Tecnologia e Ensino Superior (MCTES), from Fundo social Europeu (FSE).

Institutional Review Board Statement: Not applicable.

Informed Consent Statement: Not applicable.

Data Availability Statement: The studied cultures were deposited in the Micoteca da Universidade do Minho (MUM), Braga, Portugal. Generated DNA sequences were deposited in GenBank (see Table 1), while phylogenetic data were deposited in Figshare (10.6084/m9.figshare.27126240). The Whole Genome Shotgun project has been deposited at GenBank under the Accession Number JBHZOJ000000000 (BioProject PRJNA1167770; BioSample SAMN44013735). The version described in this manuscript is JBHZOJ010000000.

Conflicts of Interest: The authors declare no conflicts of interests.

References

1. Ferreira da Silva, E.; Zhang, C.; Serrano Pinto, L.; Patinha, C.; Reis, P. Hazard Assessment on Arsenic and Lead in Soils of Castromil Gold Mining Area, Portugal. *Appl. Geochem.* **2004**, *19*, 887–898. [CrossRef]
2. Donato, D.B.; Nichols, O.; Possingham, H.; Moore, M.; Ricci, P.F.; Noller, B.N. A Critical Review of the Effects of Gold Cyanide-Bearing Tailings Solutions on Wildlife. *Environ. Int.* **2007**, *33*, 974–984. [CrossRef] [PubMed]
3. Ngole-Jeme, V.M.; Fantke, P. Ecological and Human Health Risks Associated with Abandoned Gold Mine Tailings Contaminated Soil. *PLoS ONE* **2017**, *12*, e0172517. [CrossRef] [PubMed]
4. Crognale, S.; D'Annibale, A.; Pesciaroli, L.; Stazi, S.R.; Petruccioli, M. Fungal Community Structure and As-Resistant Fungi in a Decommissioned Gold Mine Site. *Front. Microbiol.* **2017**, *8*, 2202. [CrossRef] [PubMed]
5. Hyde, K.D.; Xu, J.; Rapior, S.; Jeewon, R.; Lumyong, S.; Niego, A.G.T.; Abeywickrama, P.D.; Aluthmuhandiram, J.V.S.; Brahamanage, R.S.; Brooks, S.; et al. The Amazing Potential of Fungi: 50 Ways We Can Exploit Fungi Industrially. *Fungal Divers.* **2019**, *97*, 1–136. [CrossRef]
6. Lücking, R.; Aime, M.C.; Robbertse, B.; Miller, A.N.; Aoki, T.; Ariyawansa, H.A.; Cardinali, G.; Crous, P.W.; Druzhinina, I.S.; Geiser, D.M.; et al. Fungal Taxonomy and Sequence-Based Nomenclature. *Nat. Microbiol.* **2021**, *6*, 540–548. [CrossRef]
7. Corbu, V.M.; Gheorghe-Barbu, I.; Dumbravă, A.Ș.; Vrâncianu, C.O.; Șesan, T.E. Current Insights in Fungal Importance—A Comprehensive Review. *Microorganisms* **2023**, *11*, 1384. [CrossRef]
8. Niego, A.G.T.; Lambert, C.; Mortimer, P.; Thongklang, N.; Rapior, S.; Grosse, M.; Schrey, H.; Charria-Girón, E.; Walker, A.; Hyde, K.D.; et al. The Contribution of Fungi to the Global Economy. *Fungal Divers.* **2023**, *121*, 95–137. [CrossRef]
9. Houbraken, J.; Kocsubé, S.; Visagie, C.M.; Yilmaz, N.; Wang, X.-C.; Meijer, M.; Kraak, B.; Hubka, V.; Bensch, K.; Samson, R.A.; et al. Classification of *Aspergillus*, *Penicillium*, *Talaromyces* and Related Genera (*Eurotiales*): An Overview of Families, Genera, Subgenera, Sections, Series and Species. *Stud. Mycol.* **2020**, *95*, 5–169. [CrossRef]
10. Bhunjun, C.S.; Chen, Y.J.; Phukhamsakda, C.; Boekhout, T.; Groenewald, J.Z.; Mckenzie, E.H.C.; Francisco, E.C.; Frisvad, J.C.; Groenewald, M.; Hurdeal, V.G.; et al. What Are the 100 Most Cited Fungal Genera? *Stud. Mycol.* **2024**, *108*, 1–412. [CrossRef]
11. Visagie, C.M.; Yilmaz, N.; Kocsubé, S.; Frisvad, J.C.; Hubka, V.; Samson, R.A.; Houbraken, J. A Review of Recently Introduced *Aspergillus*, *Penicillium*, *Talaromyces* and Other *Eurotiales* Species. *Stud. Mycol.* **2024**, *107*, 1–66. [CrossRef] [PubMed]
12. Valix, M.; Tang, J.Y.; Malik, R. Heavy Metal Tolerance of Fungi. *Miner. Eng.* **2001**, *14*, 499–505. [CrossRef]
13. Zehra, A.; Dubey, M.K.; Meena, M.; Aamir, M.; Patel, C.B.; Upadhyay, R.S. Role of *Penicillium* Species in Bioremediation Processes. In *New and Future Developments in Microbial Biotechnology and Bioengineering*; Gupta, V.K., Rodriguez-Couto, S., Eds.; Elsevier: Amsterdam, The Netherlands, 2018; pp. 247–260. ISBN 978-0-444-63501-3.
14. Bhandari, Y.; Varma, S.; Sawant, A.; Beemagani, S.; Jaiswal, N.; Chaudhari, B.P.; Vamkudoth, K.R. Biosynthesis of Gold Nanoparticles by *Penicillium rubens* and Catalytic Detoxification of Ochratoxin A and Organic Dye Pollutants. *Int. Microbiol.* **2023**, *26*, 765–780. [CrossRef] [PubMed]

15. Coelho, E.; Reis, T.A.; Cotrim, M.; Rizzutto, M.; Corrêa, B. Bioremediation of Water Contaminated with Uranium Using *Penicillium piscarium*. *Biotechnol. Prog.* **2020**, *36*, e30322. [CrossRef] [PubMed]
16. Glukhova, L.B.; Frank, Y.A.; Danilova, E.V.; Avakyan, M.R.; Banks, D.; Tuovinen, O.H.; Karnachuk, O.V. Isolation, Characterization, and Metal Response of Novel, Acid-Tolerant *Penicillium* spp. from Extremely Metal-Rich Waters at a Mining Site in Transbaikal (Siberia, Russia). *Microb. Ecol.* **2018**, *76*, 911–924. [CrossRef]
17. Sánchez-Castellón, J.; Urango-Cárdenas, I.; Enamorado-Montes, G.; Burgos-Nuñez, S.; Marrugo-Negrete, J.; Díez, S. Removal of Mercury, Cadmium, and Lead Ions by *Penicillium* sp. *Front. Environ. Chem.* **2022**, *2*, 795632. [CrossRef]
18. Sheikhloo, Z.; Salouti, M. Intracellular Biosynthesis of Gold Nanoparticles by the Fungus *Penicillium chrysogenum*. *Int. J. Nanosci. Nanotechnol.* **2011**, *7*, 102–105. [CrossRef]
19. Magdi, H.M.; Bhushan, B. Extracellular Biosynthesis and Characterization of Gold Nanoparticles Using the Fungus *Penicillium chrysogenum*. *Microsyst. Technol.* **2015**, *21*, 2279–2285. [CrossRef]
20. Trovão, J.; Soares, F.; Paiva, D.S.; Pratas, J.; Portugal, A. A Snapshot of the Microbiome of a Portuguese Abandoned Gold Mining Area. *Appl. Sci.* **2024**, *14*, 226. [CrossRef]
21. Trovão, J.; Portugal, A.; Soares, F.; Paiva, D.S.; Mesquita, N.; Coelho, C.; Pinheiro, A.C.; Catarino, L.; Gil, F.; Tiago, I. Fungal Diversity and Distribution across Distinct Biodeterioration Phenomena in Limestone Walls of the Old Cathedral of Coimbra, UNESCO World Heritage Site. *Int. Biodet. Biodegr.* **2019**, *142*, 91–102. [CrossRef]
22. White, T.; Bruns, T.; Lee, S.; Taylor, J.; Innis, M.; Gelfand, D.; Sninsky, J. Amplification and Direct Sequencing of Fungal Ribosomal RNA Genes for Phylogenetics. In *PCR Protocols: A Guide to Methods and Applications*; Innis, M., Gelfand, D., Sninsky, J.J., White, T.J., Eds.; Academic Press: New York, NY, USA, 1990; Volume 31, pp. 315–322. [CrossRef]
23. Gardes, M.; Bruns, T.D. ITS Primers with Enhanced Specificity for Basidiomycetes—Application to the Identification of Mycorrhizae and Rusts. *Mol. Ecol.* **1993**, *2*, 113–118. [CrossRef] [PubMed]
24. Liu, Y.J.; Whelen, S.; Hall, B.D. Phylogenetic Relationships among Ascomycetes: Evidence from an RNA Polymerse II Subunit. *Mol. Biol. Evol.* **1999**, *16*, 1799–1808. [CrossRef] [PubMed]
25. Hong, S.-B.; Cho, H.-S.; Shin, H.-D.; Frisvad, J.C.; Samson, R.A. Novel *Neosartorya* Species Isolated from Soil in Korea. *Int. J. Syst. Evol. Microbiol.* **2006**, *56*, 477–486. [CrossRef] [PubMed]
26. Glass, N.L.; Donaldson, G.C. Development of Primer Sets Designed for Use with the PCR to Amplify Conserved Genes from Filamentous Ascomycetes. *Appl. Environ. Microbiol.* **1995**, *61*, 1323–1330. [CrossRef]
27. Trovão, J.; Soares, F.; Tiago, I.; Portugal, A. *Talaromyces Saxoxalicus* sp. Nov., Isolated from the Limestone Walls of the Old Cathedral of Coimbra, Portugal. *Int. J. Syst. Evol. Microbiol.* **2021**, *71*, 005175. [CrossRef]
28. Altschul, S.F.; Madden, T.L.; Schäffer, A.A.; Zhang, J.; Zhang, Z.; Miller, W.; Lipman, D.J. Gapped BLAST and PSI-BLAST: A New Generation of Protein Database Search Programs. *Nucleic Acids Res.* **1997**, *25*, 3389–3402. [CrossRef]
29. Torres-Garcia, D.; Gené, J.; García, D. New and Interesting Species of *Penicillium* (Eurotiomycetes, Aspergillaceae) in Freshwater Sediments from Spain. *MycoKeys* **2022**, *86*, 103–145. [CrossRef]
30. Lee, J.-M.; Cha, J.-E.; Yoon, Y.-S.; Eom, A.-H. *Penicillium mexicanum*: An Unrecorded Fungal Species Isolated from Air Samples Collected in Korea. *Korean J. Mycol.* **2023**, *51*, 127–133. [CrossRef]
31. Katoh, K.; Standley, D.M. MAFFT Multiple Sequence Alignment Software Version 7: Improvements in Performance and Usability. *Mol. Biol. Evol.* **2013**, *30*, 772–780. [CrossRef]
32. Okonechnikov, K.; Golosova, O.; Fursov, M. UGENE team Unipro UGENE: A Unified Bioinformatics Toolkit. *Bioinformatics* **2012**, *28*, 1166–1167. [CrossRef]
33. Gouy, M.; Guindon, S.; Gascuel, O. SeaView Version 4: A Multiplatform Graphical User Interface for Sequence Alignment and Phylogenetic Tree Building. *Mol. Biol. Evol.* **2010**, *27*, 221–224. [CrossRef] [PubMed]
34. Kalyaanamoorthy, S.; Minh, B.Q.; Wong, T.K.F.; von Haeseler, A.; Jermiin, L.S. ModelFinder: Fast Model Selection for Accurate Phylogenetic Estimates. *Nat. Methods* **2017**, *14*, 587–589. [CrossRef] [PubMed]
35. Trifinopoulos, J.; Nguyen, L.-T.; von Haeseler, A.; Minh, B.Q. W-IQ-TREE: A Fast Online Phylogenetic Tool for Maximum Likelihood Analysis. *Nucleic Acids Res.* **2016**, *44*, W232–W235. [CrossRef] [PubMed]
36. Guindon, S.; Dufayard, J.-F.; Lefort, V.; Anisimova, M.; Hordijk, W.; Gascuel, O. New Algorithms and Methods to Estimate Maximum-Likelihood Phylogenies: Assessing the Performance of PhyML 3.0. *Syst. Biol.* **2010**, *59*, 307–321. [CrossRef] [PubMed]
37. Anisimova, M.; Gil, M.; Dufayard, J.-F.; Dessimoz, C.; Gascuel, O. Survey of Branch Support Methods Demonstrates Accuracy, Power, and Robustness of Fast Likelihood-Based Approximation Schemes. *Syst. Biol.* **2011**, *60*, 685–699. [CrossRef]
38. Jalili, V.; Afgan, E.; Gu, Q.; Clements, D.; Blankenberg, D.; Goecks, J.; Taylor, J.; Nekrutenko, A. The Galaxy Platform for Accessible, Reproducible and Collaborative Biomedical Analyses: 2020 Update. *Nucleic Acids Res.* **2020**, *48*, W395–W402. [CrossRef]
39. De Coster, W.; D'Hert, S.; Schultz, D.T.; Cruts, M.; Van Broeckhoven, C. NanoPack: Visualizing and Processing Long-Read Sequencing Data. *Bioinformatics* **2018**, *34*, 2666–2669. [CrossRef]
40. Kolmogorov, M.; Yuan, J.; Lin, Y.; Pevzner, P.A. Assembly of Long, Error-Prone Reads Using Repeat Graphs. *Nat. Biotechnol.* **2019**, *37*, 540–546. [CrossRef]
41. Gurevich, A.; Saveliev, V.; Vyahhi, N.; Tesler, G. QUAST: Quality Assessment Tool for Genome Assemblies. *Bioinformatics* **2013**, *29*, 1072–1075. [CrossRef]
42. Simão, F.A.; Waterhouse, R.M.; Ioannidis, P.; Kriventseva, E.V.; Zdobnov, E.M. BUSCO: Assessing Genome Assembly and Annotation Completeness with Single-Copy Orthologs. *Bioinformatics* **2015**, *31*, 3210–3212. [CrossRef]

43. Kriventseva, E.V.; Kuznetsov, D.; Tegenfeldt, F.; Manni, M.; Dias, R.; Simão, F.A.; Zdobnov, E.M. OrthoDB V10: Sampling the Diversity of Animal, Plant, Fungal, Protist, Bacterial and Viral Genomes for Evolutionary and Functional Annotations of Orthologs. *Nucleic Acids Res.* **2019**, *47*, D807–D811. [CrossRef] [PubMed]
44. Seemann, T. Barrnap 0.7: Rapid Ribosomal RNA Prediction. 2013. Available online: https://github.com/tseemann/barrnap (accessed on 8 October 2024).
45. Laslett, D.; Canback, B. ARAGORN, a Program to Detect tRNA Genes and tmRNA Genes in Nucleotide Sequences. *Nucleic Acids Res.* **2004**, *32*, 11–16. [CrossRef] [PubMed]
46. Flynn, J.M.; Hubley, R.; Goubert, C.; Rosen, J.; Clark, A.G.; Feschotte, C.; Smit, A.F. RepeatModeler2 for Automated Genomic Discovery of Transposable Element Families. *Proc. Nat. Acad. Sci. USA* **2020**, *117*, 9451–9457. [CrossRef] [PubMed]
47. Smit, A.; Hubley, R.; Green, P. RepeatMasker Open-4.0. (2013–2015). Available online: http://www.repeatmasker.org (accessed on 8 October 2024).
48. Cantalapiedra, C.P.; Hernández-Plaza, A.; Letunic, I.; Bork, P.; Huerta-Cepas, J. eggNOG-Mapper v2: Functional Annotation, Orthology Assignments, and Domain Prediction at the Metagenomic Scale. *Mol. Biol. Evol.* **2021**, *38*, 5825–5829. [CrossRef]
49. Jones, P.; Binns, D.; Chang, H.-Y.; Fraser, M.; Li, W.; McAnulla, C.; McWilliam, H.; Maslen, J.; Mitchell, A.; Nuka, G.; et al. InterProScan 5: Genome-Scale Protein Function Classification. *Bioinformatics* **2014**, *30*, 1236–1240. [CrossRef]
50. Blum, M.; Chang, H.-Y.; Chuguransky, S.; Grego, T.; Kandasaamy, S.; Mitchell, A.; Nuka, G.; Paysan-Lafosse, T.; Qureshi, M.; Raj, S.; et al. The InterPro Protein Families and Domains Database: 20 Years On. *Nucleic Acids Res.* **2021**, *49*, D344–D354. [CrossRef]
51. Conesa, A.; Götz, S.; García-Gómez, J.M.; Terol, J.; Talón, M.; Robles, M. Blast2GO: A Universal Tool for Annotation, Visualization and Analysis in Functional Genomics Research. *Bioinformatics* **2005**, *21*, 3674–3676. [CrossRef]
52. Götz, S.; García-Gómez, J.M.; Terol, J.; Williams, T.D.; Nagaraj, S.H.; Nueda, M.J.; Robles, M.; Talón, M.; Dopazo, J.; Conesa, A. High-Throughput Functional Annotation and Data Mining with the Blast2GO Suite. *Nucleic Acids Res.* **2008**, *36*, 3420–3435. [CrossRef]
53. Zheng, J.; Ge, Q.; Yan, Y.; Zhang, X.; Huang, L.; Yin, Y. dbCAN3: Automated Carbohydrate-Active Enzyme and Substrate Annotation. *Nucleic Acids Res.* **2023**, *51*, W115–W121. [CrossRef]
54. Blin, K.; Shaw, S.; Augustijn, H.E.; Reitz, Z.L.; Biermann, F.; Alanjary, M.; Fetter, A.; Terlouw, B.R.; Metcalf, W.W.; Helfrich, E.J.N.; et al. antiSMASH 7.0: New and Improved Predictions for Detection, Regulation, Chemical Structures and Visualisation. *Nucleic Acids Res.* **2023**, *51*, W46–W50. [CrossRef]
55. Kanehisa, M.; Sato, Y.; Morishima, K. BlastKOALA and GhostKOALA: KEGG Tools for Functional Characterization of Genome and Metagenome Sequences. *J. Mol. Biol.* **2016**, *428*, 726–731. [CrossRef] [PubMed]
56. Song, X.; Li, Y.; Stirling, E.; Zhao, K.; Wang, B.; Zhu, Y.; Luo, Y.; Xu, J.; Ma, B. AsgeneDB: A Curated Orthology Arsenic Metabolism Gene Database and Computational Tool for Metagenome Annotation. *NAR Genom. Bioinform.* **2022**, *4*, lqac080. [CrossRef]
57. Buchfink, B.; Xie, C.; Huson, D.H. Fast and Sensitive Protein Alignment Using DIAMOND. *Nat. Methods* **2015**, *12*, 59–60. [CrossRef]
58. Tang, D.; Chen, M.; Huang, X.; Zhang, G.; Zeng, L.; Zhang, G.; Wu, S.; Wang, Y. SRplot: A Free Online Platform for Data Visualization and Graphing. *PLoS ONE* **2023**, *18*, e0294236. [CrossRef]
59. Visagie, C.M.; Hirooka, Y.; Tanney, J.B.; Whitfield, E.; Mwange, K.; Meijer, M.; Amend, A.S.; Seifert, K.A.; Samson, R.A. *Aspergillus*, *Penicillium* and *Talaromyces* Isolated from House Dust Samples Collected Around the World. *Stud. Mycol.* **2014**, *78*, 63–139. [CrossRef]
60. Park, M.S.; Oh, S.-Y.; Fong, J.J.; Houbraken, J.; Lim, Y.W. The Diversity and Ecological Roles of *Penicillium* in Intertidal Zones. *Sci. Rep.* **2019**, *9*, 13540. [CrossRef]
61. Wijayawardene, N.N.; Phillips, A.J.L.; Tibpromma, S.; Dai, D.Q.; Selbmann, L.; Monteiro, J.S.; Aptroot, A.; Flakus, A.; Rajeshkumar, K.C.; Coleine, C. Looking for the Undiscovered Asexual Taxa: Case Studies from Lesser Studied Life Modes and Habitats. *Mycosphere* **2021**, *12*, 1290–1333. [CrossRef]
62. Coleine, C.; Stajich, J.E.; Selbmann, L. Fungi Are Key Players in Extreme Ecosystems. *Trends Ecol. Evol.* **2022**, *37*, 517–528. [CrossRef]
63. Petersen, C.; Sørensen, T.; Nielsen, M.R.; Sondergaard, T.E.; Sørensen, J.L.; Fitzpatrick, D.A.; Frisvad, J.C.; Nielsen, K.L. Comparative Genomic Study of the *Penicillium* Genus Elucidates a Diverse Pangenome and 15 Lateral Gene Transfer Events. *IMA Fungus* **2023**, *14*, 3. [CrossRef]
64. Visagie, C.M.; Magistà, D.; Ferrara, M.; Balocchi, F.; Duong, T.A.; Eichmeier, A.; Gramaje, D.; Aylward, J.; Baker, S.E.; Barnes, I.; et al. IMA Genome-F18. *IMA Fungus* **2023**, *14*, 21. [CrossRef]
65. Roxo, I.; Amaral, A.; Portugal, A.; Trovão, J. Draft Genome Sequence and Comparative Genomic Analysis of *Penicillium pancosmium* MUM 23.27 Isolated from Raw Honey. *Arch. Microbiol.* **2024**, *206*, 36. [CrossRef] [PubMed]
66. Coleine, C.; Masonjones, S.; Sterflinger, K.; Onofri, S.; Selbmann, L.; Stajich, J.E. Peculiar Genomic Traits in the Stress-Adapted Cryptoendolithic Antarctic Fungus *Friedmanniomyces endolithicus*. *Fungal Biol.* **2020**, *124*, 458–467. [CrossRef] [PubMed]
67. Paiva, D.S.; Fernandes, L.; Portugal, A.; Trovão, J. First Genome Sequence of the Microcolonial Black Fungus *Saxispiralis lemnorum* MUM 23.14: Insights into the Unique Genomic Traits of the *Aeminiaceae* Family. *Microorganisms* **2024**, *12*, 104. [CrossRef] [PubMed]
68. Pao, S.S.; Paulsen, I.T.; Saier, M.H. Major Facilitator Superfamily. *Microbiol. Mol. Biol. Rev.* **1998**, *62*, 1–34. [CrossRef] [PubMed]
69. Vaccaro, F.A.; Drennan, C.L. The Role of Nucleoside Triphosphate Hydrolase Metallochaperones in Making Metalloenzymes. *Metallomics* **2022**, *14*, mfac030. [CrossRef]

70. Zhang, S.; Shi, G.; Xu, X.; Guo, X.; Li, S.; Li, Z.; Wu, Q.; Yin, W.-B. Global Analysis of Natural Products Biosynthetic Diversity Encoded in Fungal Genomes. *J. Fungi* **2024**, *10*, 653. [CrossRef]
71. Morales-Oyervides, L.; Ruiz-Sánchez, J.P.; Oliveira, J.C.; Sousa-Gallagher, M.J.; Méndez-Zavala, A.; Giuffrida, D.; Dufossé, L.; Montañez, J. Biotechnological Approaches for the Production of Natural Colorants by *Talaromyces/Penicillium*: A Review. *Biotechnol. Adv.* **2020**, *43*, 107601. [CrossRef]
72. Afroz Toma, M.; Rahman, M.H.; Rahman, M.S.; Arif, M.; Nazir, K.H.M.N.H.; Dufossé, L. Fungal Pigments: Carotenoids, Riboflavin, and Polyketides with Diverse Applications. *J. Fungi* **2023**, *9*, 454. [CrossRef]
73. Bignell, E.; Cairns, T.C.; Throckmorton, K.; Nierman, W.C.; Keller, N.P. Secondary Metabolite Arsenal of an Opportunistic Pathogenic Fungus. *Philos. Trans. R. Soc. Lond. B Biol. Sci.* **2016**, *371*, 20160023. [CrossRef]
74. Ries, M.I.; Ali, H.; Lankhorst, P.P.; Hankemeier, T.; Bovenberg, R.A.L.; Driessen, A.J.M.; Vreeken, R.J. Novel Key Metabolites Reveal Further Branching of the Roquefortine/Meleagrin Biosynthetic Pathway. *J. Biol. Chem.* **2013**, *288*, 37289–37295. [CrossRef]
75. Banani, H.; Marcet-Houben, M.; Ballester, A.-R.; Abbruscato, P.; González-Candelas, L.; Gabaldón, T.; Spadaro, D. Genome Sequencing and Secondary Metabolism of the Postharvest Pathogen *Penicillium griseofulvum*. *BMC Genom.* **2016**, *17*, 19. [CrossRef] [PubMed]
76. Garello, M.; Piombo, E.; Buonsenso, F.; Prencipe, S.; Valente, S.; Meloni, G.R.; Marcet-Houben, M.; Gabaldón, T.; Spadaro, D. Several Secondary Metabolite Gene Clusters in the Genomes of Ten *Penicillium* spp. Raise the Risk of Multiple Mycotoxin Occurrence in Chestnuts. *Food Microbiol.* **2024**, *122*, 104532. [CrossRef]
77. Fujii, I.; Yasuoka, Y.; Tsai, H.-F.; Chang, Y.C.; Kwon-Chung, K.J.; Ebizuka, Y. Hydrolytic Polyketide Shortening by Ayg1p, a Novel Enzyme Involved in Fungal Melanin Biosynthesis. *J. Biol. Chem.* **2004**, *279*, 44613–44620. [CrossRef] [PubMed]
78. Pohl, C.; Polli, F.; Schütze, T.; Viggiano, A.; Mózsik, L.; Jung, S.; de Vries, M.; Bovenberg, R.A.L.; Meyer, V.; Driessen, A.J.M. A *Penicillium rubens* Platform Strain for Secondary Metabolite Production. *Sci. Rep.* **2020**, *10*, 7630. [CrossRef] [PubMed]
79. Piras, M.; Patruno, I.; Nikolakopoulou, C.; Willment, J.A.; Sloan, N.L.; Zanato, C.; Brown, G.D.; Zanda, M. Synthesis of the Fungal Metabolite YWA1 and Related Constructs as Tools to Study MelLec-Mediated Immune Response to *Aspergillus* Infections. *J. Org. Chem.* **2021**, *86*, 6044–6055. [CrossRef]
80. Park, Y.-I.; Gander, J.E. Choline Derivatives Involved in Osmotolerance of *Penicillium fellutanum*. *Appl. Environ. Microbiol.* **1998**, *64*, 273–278. [CrossRef]
81. Markham, P.; Robson, G.D.; Bainbridge, B.W.; Trinci, A.P.J. Choline: Its Role in the Growth of Filamentous Fungi and the Regulation of Mycelial Morphology. *FEMS Microbiol. Rev.* **1993**, *10*, 287–300. [CrossRef]
82. Cordero, R.J.B.; Vij, R.; Casadevall, A. Microbial Melanins for Radioprotection and Bioremediation. *Microb. Biotechnol.* **2017**, *10*, 1186–1190. [CrossRef]
83. Gostinčar, C.; Muggia, L.; Grube, M. Polyextremotolerant Black Fungi: Oligotrophism, Adaptive Potential, and a Link to Lichen Symbioses. *Front. Microbiol.* **2012**, *3*, 390. [CrossRef]
84. Morawe, M.; Hoeke, H.; Wissenbach, D.K.; Lentendu, G.; Wubet, T.; Kröber, E.; Kolb, S. Acidotolerant Bacteria and Fungi as a Sink of Methanol-Derived Carbon in a Deciduous Forest Soil. *Front. Microbiol.* **2017**, *8*, 1361. [CrossRef]
85. Gou, J.; Xia, J.; Li, Y.; Qiu, Y.; Jiang, F. A Novel Sulfidogenic Process via Sulfur Reduction to Remove Arsenate in Acid Mine Drainage: Insights into the Performance and Microbial Mechanisms. *Water Res.* **2024**, *254*, 121423. [CrossRef] [PubMed]
86. Johnson, L. Iron and Siderophores in Fungal-Host Interactions. *Mycol. Res.* **2008**, *112*, 170–183. [CrossRef] [PubMed]
87. Xie, B.; Wei, X.; Wan, C.; Zhao, W.; Song, R.; Xin, S.; Song, K. Exploring the Biological Pathways of Siderophores and Their Multidisciplinary Applications: A Comprehensive Review. *Molecules* **2024**, *29*, 2318. [CrossRef]
88. Fomina, M.; Gadd, G.M. Biosorption: Current Perspectives on Concept, Definition and Application. *Bioresour. Technol.* **2014**, *160*, 3–14. [CrossRef] [PubMed]
89. Gadd, G.M. Geomycology: Biogeochemical Transformations of Rocks, Minerals, Metals and Radionuclides by Fungi, Bioweathering and Bioremediation. *Mycol. Res.* **2007**, *111*, 3–49. [CrossRef]
90. Gadd, G.M. Metals, Minerals and Microbes: Geomicrobiology and Bioremediation. *Microbiology* **2010**, *156*, 609–643. [CrossRef]

Disclaimer/Publisher's Note: The statements, opinions and data contained in all publications are solely those of the individual author(s) and contributor(s) and not of MDPI and/or the editor(s). MDPI and/or the editor(s) disclaim responsibility for any injury to people or property resulting from any ideas, methods, instructions or products referred to in the content.